International Journal of Advanced Engineering and Management Research
Vol. 2 Issue 5, 2017

http://ijaemr.com/ ISSN: 2456-3676

SYNTHESIS OF OPEN CELL ALUMINIUM FOAMS

AbarcaPatricio; Díaz Carlos,SotomayorOscar[1]

[1]Escuela Politécnica Nacional, Facultad de Ingeniería Mecánica, Quito, Ecuador

ABSTRACT

In the present study samples of aluminium foams of open cell were obtained by the method of infiltration of molten metal in soluble NaCL perform with a grain size in the range of 0.85-1.7 mm. These samples were subsequently characterized structurally and mechanically. The foam samples were fabricated based on an experimental protocol of infiltration relatively easy to implement and replicate in the Metal Casting Laboratory at EPN. Regarding the structural characterization, parameters such as relative density, pore size, percentage of porosity and others were studied. All these parameters were analyzed statistically. Results suggest that the samples are not totally homogeneous, since in the majority there is a considerable standard deviation. The mean value of porosity in the samples analyzed was 85.5%, indicating the production of a highly porous foam. The presence of pores with sizes above the established range of NaCl grains (0.85-1.7 mm) could indicate particle sintering, probably due to some excess temperature in the process. With respect to the mechanical characterization, the compression test was performed on a representative sample, in which it is observed that the extended plateau area of the stress-strain curve presents a slight positive slope, characteristic of this type of materials, which may be the result of the constant deformation hardening of the foam. The values obtained from the calculation of the absorbed compressive energy, verify the high capacity of absorption of energy of deformation, in these materials.

Key Words: metal foam, open cell, infiltration, porosity.

1. INTRODUCTION

Metallic foams are interesting materials from the technological point of view, mainly because of their combination of low weight and high strength, high capacity of energy absorption, and high permeability, among others; which provides a wide variety of applications in engineering (Nebreda, 2014). In addition, they enable various ranges of mechanical, acoustic and thermal properties, which are suggestive in the design of ultra-lightweight structures, high impact

resistance elements, acoustic insulation elements, heat dissipation and filters (Fernández, Cruz, & García, 2009).

Some macroscopic features of their structure (pore size, cell type, cell wall curvature, specific density, among others) have a marked influence on mechanical response, and can be relatively controlled by processing techniques that are mostly very complex and expensive(Gutiérrez & Oñoro, 2008). Although great progress has been made in interpreting the structure-property relationship of metal foams, the large number of different techniques produce materials with different characteristics and structures, which means that the understanding of the proper control of the parameters in the processes of obtaining metallic foams is still insufficient (Luna, Barari, Woolle, & Goodall, 2014).

In this work it has been considered substantial to carry out a study on the synthesis of open cell aluminum foams in which an economical and efficient method is applied to obtain foams susceptible of control over their structure and morphology. In addition, also characterize the metallic foams obtained structurally and mechanically, in order to be a contribution to the database available today on the subject.

Based on studies performed, such as:Luna, Barari, Woolle y Goodall (2014), Hussain y Suffin, (2011), Fernández (2007), Xiaoqing, Zhihua, Hongwei, Longmao, y Guitong (2006),Fernández, Daza, Oviedo, Ortega, & Cruz (2009), Fernández, Cruz, & García (2009), among others; open cell aluminium foams have been characterized which were obtained by the infiltration method, in where the perform removed by dissolution in water was sodium chloride (NaCl).This method was chosen because of its relative experimental simplicity and because, according to reports of other authors, it can offer a high degree of control over the final structure of the foams(Banhart, 2000). In addition, the costs of the raw material used are not relevant, and compared to the other known production processes, it is evidenced as a more economical, simple and practical process (Roldán & Angel, 2012).

2. METHODOLOGY

2.1Materials and equipment

The process to be used is based on the infiltration of molten aluminium around a preform of particles of NaCl that defines the final porosity of material. The basic infiltration process for obtaining open-cell metal foams is illustrated in Figure 1.

In the present work, the process to obtain the open cell metal foam by the infiltration method is based on the experimental protocole developed and published by Luna, Barari, Woolle and Goodall (2014), from Department of Science and Materials Engineering at the University of Sheffield. This protocol was modified in part, first according to certain needs presented during the experiments, and second, in order to adapt the process of obtaining to the elements available in the laboratory used. The protocol developed is relatively easy to implement in any research laboratory (Figure 2).

2.2 Experimental process

The process begins by obtaining a number of cylindrical aluminium bars, with a diameter of 50 mm, which is slightly smaller than the internal diameter of 51 mm of the cylindrical chamber to be used in the infiltration. These bars, once obtained, are sectioned into pieces of 3 or 4 cm in length (this size depends on the amount of NaCl to be infiltrated), these pieces are the aluminium billets that are used for infiltration. The bars were obtained by means of the casting process in closed sand mold, whose internal cylindrical cavity had a diameter of 52 mm in order to compensate for contraction effects of the metal. Subsequently, if the diameter of the bar obtained is not 50 mm, it must be machined to the desired value.

The cylindrical mold used is composed of the elements shown in Figure 3. The material of such elements is AISI 304 stainless steel. The cylindrical chamber must be free of any obvious impurity prior to use, taking special consideration at both edges of the top and bottom; for this you can use sandpaper.

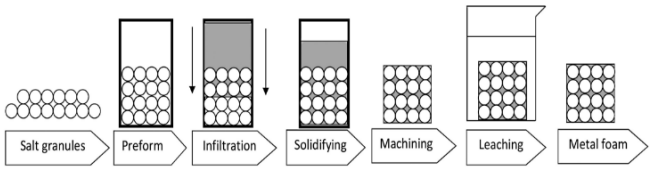

Figure1. General steps of the replication process to obtain open cell metal foam.

(Source: Luna, Barari, Woolle, & Goodall, 2014)

Subsequently a coating of graphite powder was applied to the inner surface of the cylindrical mold, creating a thin layer, in order to facilitate the extraction of the foam sample produced (another option would be to spray the inner surface of the mold with aerosol of boron nitride, and / or manufacture a mold with a small degree of conicity on the inner surface thereof).

It is important that the cylindrical mold remain airtight during the experiment, for which 2 rings of graphite sheet were cut with the following measures: thickness = 2 mm, external diameter = 60mm, internal diameter = 51mm.These rings acting as sealing material were each respectively located in the grooves of the mold caps (Figure 3b).

a)

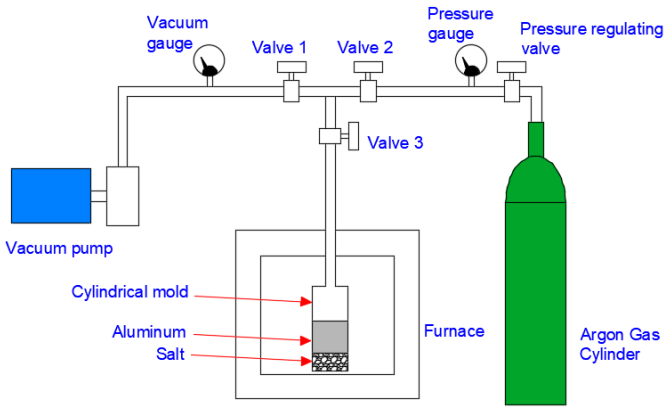

b)

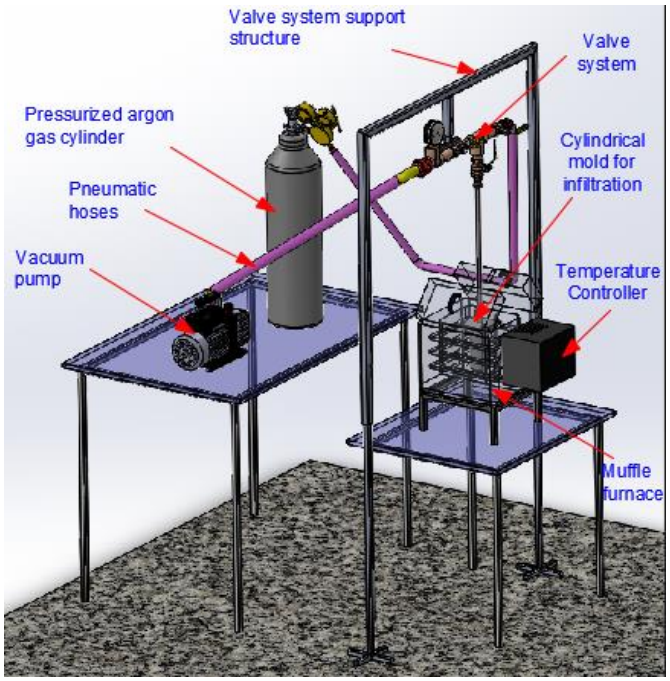

Figure2.(a) Schematic of the equipment to obtain metallic foams of open cell. (b) Modeling of the materials and equipment assembled to obtain the metal foam.

Taking into account that the melting temperature of the aluminium is 660 ° C and that of the NaCl is 801 ° C, one of the required parameters is that the temperature inside the cylindrical mold be around 740 ° C, since it would allow an adequate infiltration of the aluminium through the interstitial spaces of the grains of NaCl, without these grain smelting. The thermocouple of the muffle furnace only measures the room temperature inside it, and this value is not necessarily the temperature at which the interior of the cylindrical mold is located. Therefore, an iterative

method is applied, in order to program gradually several Values of temperature in the furnace, and with each of them, by means of the use of a pyrometer (calibrated with an emissivity of 0.59 for stainless steel), it is verified the temperature that reaches the external wall of a replica cylinder, made of the same material that the cylindrical mold (this temperature must be approximate to the temperature inside the mold).After a series of tests, the infiltration gave acceptable results, when the temperature recorded by the pyrometer on the outer wall of the replica cylinder stabilized at approximately 800 °C, such temperature was achieved when the muffle oven was programmed to reach 340 °C for at least 2 h, sufficient time further to properly preheat the furnace. The heating rate of the furnace was set at 20 °C/min.

With respect to the preform, the size of grains of salt (NaCl) in the range of 0.85 to 1.7 mm (pore size required for the foam) was selected through a sifting process.mSubsequently it was used 200 g (this value depends on the foam size required) of sifted salt for infiltration.

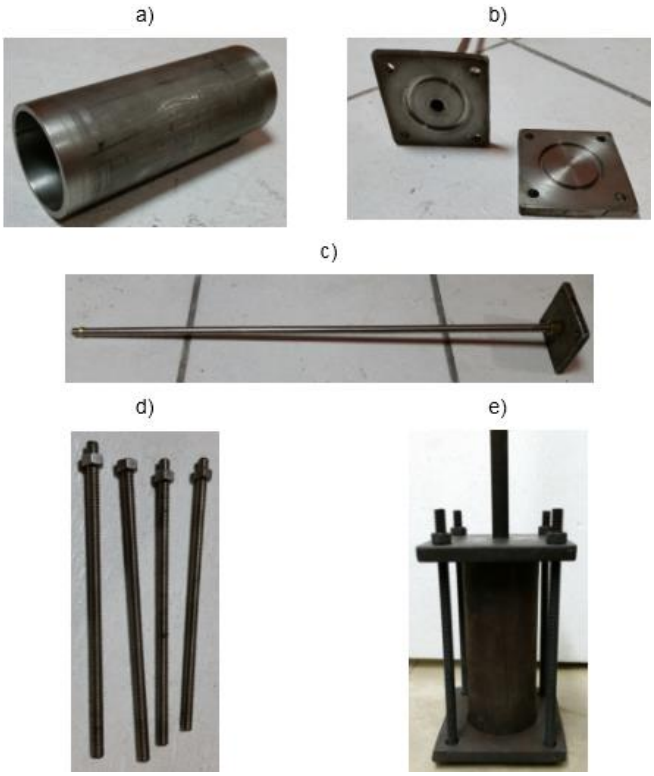

Figura 3.Cylindrical mold. (a) Cylindrical chamber. (b) Top and bottom slotted cylindrical caps. (c) Duct adapted to the top of the cylindrical chamber and connected to the valve system. (d) Threaded rods that allow rigid coupling the upper and lower caps to the cylindrical chamber.(e) Fully assembled cylindrical mold.

Once the cylinder is located inside the groove of the lower lid of the mold, the sieved NaCl grains are poured and carefully shaken in such a way that the grains in the upper part of the

cylinder form a flat surface. Subsequently, the prepared aluminium billet is placed in the upper part of the NaCl perform. The upper cover is then mounted on the threaded rods, and the nuts are tightened tightly to seal the mold (Figure 3e).

For the transmission of the negative and positive pressure respectively required in the process, the assembled mold is coupled to the valve system. M Negative pressure is required to verify the seal between the caps and the mold cylinder, further extracting the air from the chamber, will be treated of avoid oxidation of the aluminium, otherwise increase the viscosity of the cast, resulting in greater difficulty for infiltration. The positive pressure helps the aluminium to infiltrate all the interstitial spaces that exist between the grains of salt.

Once the valve system is coupled to the cylindrical mold, all the valves in the system are closed, and only the valves connecting the vacuum pump and the mold are opened, in this case valves 3 and 1(Figure 2a). The vacuum pump turns on until the vacuum gauge indicates the lowest possible pressure (in this case the recorder pressure was -0.65 bar).The pump is shut down, and if the vacuum loss in the system is less than 50 Torr / s (0.0666 Bar / s) for the first 10 seconds after the vacuum pump is turned off, the seal is appropriate for infiltration. Valve 3 is left open to keep the system at ambient pressure and valve 1 is closed(Figure 2a). Without separating the valve system, place the mold in the preheated oven and wait for 1 h.

Afterwards, all valves in the system are closed, valve 2 is opened which leads to the argon gas tank (Figure 2a), the main valve of the said tank is opened and the infiltration pressure is established with the pressure regulating valve (the pressure used was of 3.5 bar = 50.76 psi, with NaCl grains size between a range of 0.85 mm to 1.7 mm). Quickly open the valve 3, and after 1 min, remove the mold from the oven and place it on top of a cooling surface, in this case a metal surface to accelerate the loss of heat.

After 30 minutes, when the mold is cold enough to handle it lightly with heat resistant gloves, disconnect the valve system and separate the cylinder from the mold of the upper and lower caps, place it in the grip of a screw press, and by hammering on the remaining aluminium remaining not infiltrated in the top of the sample, push the sample out of the mold cylinder.

Place the infiltrated foam in a container with water exposed to the flame and allow to boil until the NaCl preform is dissolved; change the water every 10 minutes until completely remove the NaCl from the foam (change the water approximately 10 times).Using a band saw, cut the bottom of the foam sample, removing excess non-infiltrated aluminium (Figure 4a).

3. RESULTS AND DISCUSSION

3.1 Structural characterization

To initiate the structural characterization, the obtained samples were required to be sectioned, this because the cylindrical periphery of the same did not offer more details for an adequate analysis. In order to minimize the distortion of the ligaments, the sectioning was carried out by electrical-discharge wire cutting (wire EDM) process. To provide a good finish to facilitate analysis, the flat surfaces of the sectioned samples were polished using fine abrasive paper to avoid damage (1000 gauge sandpaper) (Figure 4b). Once the surfaces of the samples were prepared, each was observed using an optical microscope with a magnification of 4x, where the necessary photographs were taken for subsequent image analysis in CAD software. All photographs show a reference length of 0.2 in the lower right (Figure 4b), this was used to obtain the measurements required in the different parameters analyzed. It should be clarified that the results of certain parameters will be only approximations, since they come from a two dimensional image analysis.

a)

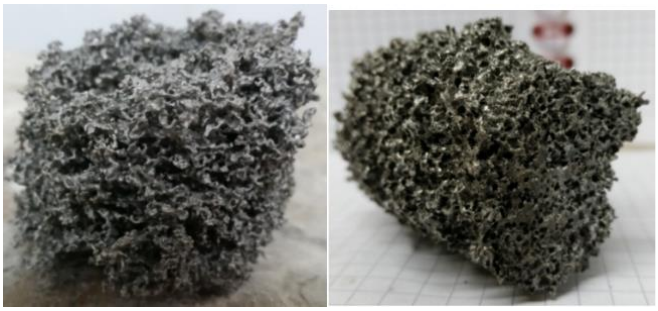

b)

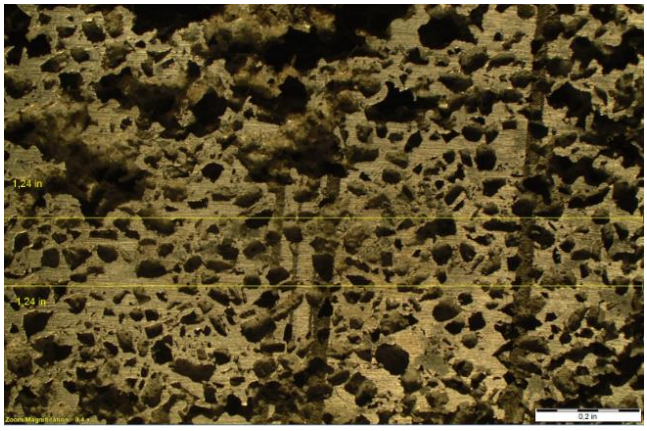

Figure 4.(a) Samples from which the NaCl grains were dissolved and the surplus aluminium that was not infiltrated was removed. (b) Photograph of one of the samples of open cell metal foam, which have been sectioned, polished and observed under an optical microscope at 4x.

Data collection was performed using a sampling procedure; this data was studied statistically and average values for six samples and more than fifty measurements per sample.

- *Pores per inch (PPI).*

It has a total mean value of 18 pores per inch, and a standard deviation of 2.67, which indicates that the number of pores per inch does not differ greatly in each sample. Hence it remains closely uniform.

- *Ligament thickness.*

Data can be associated in three major percentages: (a) approximately 28.42% of ligaments that are in a thickness range of 200-300 μm, with a standard deviation of 8.47%. (b) Approximately 23.68%, are in a thickness range of 100-200 μm, with a standard deviation of 17.38%. (c) Approximately 20%, are in a thickness range of 300-400 μm, with a standard deviation of 7.91%. The remaining of ligaments are scattered in different ranges. These results indicate that most of the ligament thickness (72.1%) are in the total range of 100-400 μm, which is a very broad range, and this added to the fact that the standard deviation in each range analyzed is considerable, it is concluded that the thickness of ligaments between pores of the samples is very broad.

- *Surface pore size.*

There are three major percentages of pore sizes registered: (a) approximately 29.78% of pores are in a superficial range of 1×10^5 - $3 \times 10^5 \mu m^2$, with a standard deviation of 22.1%, (b) approximately 22.47% of pores are in a superficial range of 3×10^5 - $5 \times 10^5 \mu m^2$, with a standard deviation of 13.76%, and (c) approximately 20.79% of pores, are in a superficial range of 5×10^5 - $7 \times 10^5 \mu m^2$, with a standard deviation of 14.79%. The remaining pores are scattered in different ranges. These results indicate that most of the surface pore size (73.04%) are in the range of 1×10^5- $7 \times 10^5 \mu m^2$, which is very broad.

- *Pore length.*

Are registered two major percentages: (a) approximately 36.72% of pores, are in a length range of 500 - 1000 μm, with a standard deviation of 18.62%, and (b) approximately 36,72% of pores, are in a range of 1000 - 1500 μm, with a standard deviation of 12.39%. The remaining pores are scattered in different ranges. These results indicate that most of the longitudinal size of pore (73.44%) are in the range of 500 - 1500 μm.

- *Pore width.*

Two major percentages are recorded: (a) approximately 32.39% of pores are in a range width of 300-600 μm, with a standard deviation of 12.71%, and (b) approximately 34.09 % of pores, are in a range of 600-900 μm, with a standard deviation of 6.1%. The remaining pores are scattered in different ranges. These results indicate that most of the pore width (66.48%) are in the range of 300 - 900 μm.

- *Anisotropy.*

Anisotropy is related with pores that tend to be elongated in some direction(Laughlin & Hono, 2014). Hence, it is directly influenced by pore's width / long ratio. While this relationship is closer to one, it is understood that the behavior will be isotropic. The regular pores that contribute to an isotropic behavior to the foam are approximately 21.02% which have a width / long ratio range of 0.8-1, with a standard deviation of 11.89%. These results indicate that the amount of anisotropic pores, far exceeds the isotropic ones, therefore, it is considered that the foams would have anisotropic behavior.

If the metal foam exhibits a tendency for pore elongation in any particular direction, the response of the foam will likewise exhibit a directional mechanical response. Therefore, one of the samples obtained was analyzedin order to define the directional tendency of the pores. The counter clockwise angle between a symmetrical axis in the pore and a horizontal line was measured in a CAD software. The horizontal line has been chosen so that it corresponds to the plane perpendicular to infiltration. These results indicate that most of the pores (approximately 59.2%) have a tendency of inclination between 90° and 150° which slightly corresponds to the direction of the infiltration.

- *Pore shape.*

A pore can be considered approximately equiaxial if the width / long ratio is close to or equal to one(Banhart, 2000). Therefore, the pores that could be considered approximately equiaxial represent only 21.02% with a standard deviation of 11.89%, and are in a width / long ratio range of 0.8-1. These results indicate that the amount of non-equiaxial pores, far exceeds those that are equiaxial, consequently, it could be established that the foams in general would be composed of non-equiaxial pores.

- *Porosity.*

Porosity (or relative density) is one of the most important parameters of a metal foam. The porosity, degree of expansion and relative density are reported in a Table 1. The formulae for calculation of the parameters is defined as(Gibson & Ashby, 2007):

$$\rho_r = \frac{\rho}{\rho_s} \qquad (1)$$

$$p \approx 1 - \frac{\rho}{\rho_s} = 1 - \rho_r \qquad (2)$$

$$G = \frac{V}{V_s} = \frac{\rho_s}{\rho} = \frac{1}{\rho_r} \quad (3)$$

Where:

$\rho_r = Relative\ density$

$\rho = Density\ of\ cellular\ material$

$\rho_s = Density\ of\ base\ material$

$p = Porosity$

The metal foams obtained by infiltration, in which it was used a NaCl particle size of 0.85 - 1.7 mm, have an average porosity value of 85.5% (Table 1), indicating that the foams have relatively high levels of porosity or low relative density.

Table 1. Data of relative density, porosity and degree of expansion of three metal foam samples obtained by the infiltration method.

Sample	Particle size (mm) of NaCl used as preform	Relative density	Porosity	Porosity (%)	Expansion grade	Expansion grade (%)
1	0,85 – 1,7	0,124	0,876	87,6	8,065	806,452
2	0,85 – 1,7	0,165	0,835	83,5	6,061	606,061
3	0,85 – 1,7	0,146	0,854	85,4	6,849	684,932
	Mean	0,145	**Mean**	85,5	**Mean**	699,148
	Standard deviation	0,0205	**Standard deviation**	2,052	**Standard deviation**	100,949

In the research carried out by other authors(Luna, Barari, Woolle, & Goodall, 2014), for a particle size of NaCl in the range of 1.4 - 1.7 mm, the recorded porosity has an average value of 63.2%. It is suggested that the level of porosity is directly influenced by the size of NaCl particles. The smaller the size of the particles the higher the porosity. As it have been suggested by other authors (Hussain & Suffin, 2011), with smaller sizes of NaCl particles the pores will have more closely spaced, and therefore their cell walls and ligaments will tend to be thinner. Figure 5a shows the variation of ligament thickness that can be found in the foam.

Another important aspect affecting the degree of porosity in the foams is the sintering of particles or NaCl grains, which may occur when the temperature during the foaming process exceeds the melting temperature of the salt (801 ° C) (Fernández, 2007). Such sintering leads to the formation of agglomerates, where each behaves as a single large dimensions particle. This, after the infiltration of the aluminium, will cause the appearance of pores or holes in the foam that replicate the size of agglomerates (Fernández, 2007). This is undesirable since there would be no regular structure in the foam. Figure 5b shows the length of certain pores, which greatly exceed the particle size range of NaCl (0.85 - 1.7 mm) used in the experiment, this could be due to the agglomeration of the particles already indicated.

It should be mentioned that even without reaching the NaCl melting temperature, it is possible that some agglomeration of the grains of salt are produced (Fernández, 2007). Moreover, in Figure 5b it can be seen that there are also pores that are smaller than the range of particle size used during experiment. This could be explained by fact that some smaller particles are present after sieving (<0.85 mm). A possible solution for this could be to increase the time of sieving and / or decrease the amount of NaCl for each sieving operation. The small pores could generate contact points between grains, which after the dissolution of NaCl, allow the interconnection between pores (Fernández, 2007). These contact points are responsible for the NaCl particles not being isolated, rather they are allowed to dissolve and as a result the open cell structure is obtained in the foam. Figure 6 illustrates this phenomena. The thickness of certain ducts are in the range of 120 to 224 μm (see figure 6b).

a)

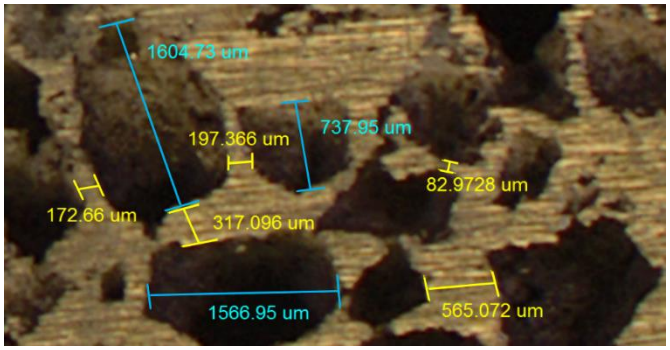

b)

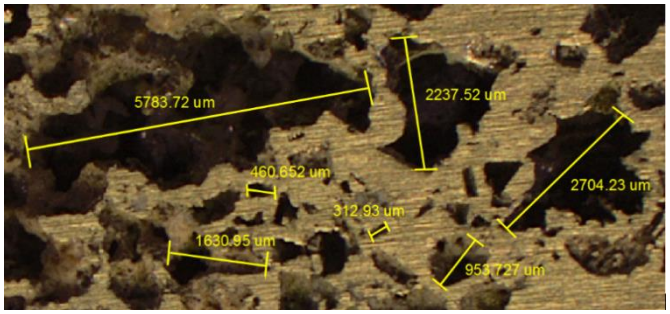

Figure5.(a) Random magnified view of a fraction of one of the samples, where it can be seen that there are different thicknesses of ligament between pores (yellow dimensions belong to the thickness of ligaments between pores, blue dimensions belong to the length of the pore). (b) Enlarged view of a fraction of one of the samples, where large pores are observed, which exceed well above the particle size range (0.85 - 1.7 mm) used in the experiment. On the other hand, pores smaller than the mentioned range can also be observed.

3.2 Uniaxial compression test.

A representative uniaxial compression test is performed on one of the cylindrical specimens of metal foam obtained, having a height (H) of 51.04 mm and a diameter (D) of 36.6 mm, giving a H/D ratio of 1.4.As a result it was found that the height of the specimen was reduced to approximately 8.18 mm, and its diameter increased to approximately 52.96 mm (Table 2).

The stress-strain curve of a compression test in a metallic foam can usually present three regions respectively: elastic linear region (or elastic zone), extended plateau region with almost constant stress, and densification region when the collapsed pores are compacted together (Xiaoqing, Zhihua, Hongwei, Longmao, & Guitong, 2006). With the values of stress and unit strain obtained from the deformation and applied load measurements that were recorded in the uniaxial compression test, it is clear that the elastic zone could not be defined (Figure 7), this is due to the fact that an strain gauge is difficult to place on the metallic foam. As a consequence, sensing the small deformations of the elastic range is a challenge and have not been registered in the universal testing machine at EPN.The second region has a slight positive slope (see Figure 7), characteristic of this type of materials, which can be the result of the hardening by constant deformation that the foam undergoes, due to the rearrangement of its structure, during the process of deformation (Fernández, Daza, Oviedo, Ortega, & Cruz, 2009).The densification is located from 0.6 onwards (Figure 7), in this range the curve begins to grow abruptly. This densification is the product of the settlement of the cellular structure that begins during the deformation, where the pore edges gradually occupy the space between the pores (Fernández, Cruz, & García, 2009).

Table 2. Initial and final data of the geometry and load recorded on the open cell metal foam specimen subjected to the uniaxial compression test.

Sample	Initial measure	Final measurement	Percentage (%)
Length	51,04 mm	8,18 mm	It reduced by 84%
Diameter	36,6 mm	52,96 mm	It increased by 44.7%
Cross-sectional area	1052,09 mm^2 (0,001052 m^2)	2202,85 mm^2 (0,002203 m^2)	
Registered charge	0	66583 N	

Since an important application for metal foams is impact absorption, it is relevant to determine the compressive energy absorbed by the foam subjected to the compression test. The amount of compressive energy absorbed is defined as the area under the strain-strain curve(Xiaoqing, Zhihua, Hongwei, Longmao, & Guitong, 2006), calculate by:

$$W = \int_0^{\varepsilon_m} \sigma(\varepsilon) d\varepsilon \quad (5)$$

Where : $\sigma(\varepsilon) = Equation\ of\ the\ curve\ as\ a\ function\ of\ the\ unit\ deformation W$

It is evident that the area under the curve located before the densification zone (Figure 7a) represents the most readily absorbed energy since a large deformation has occurred with relatively small levels of stress. In contrast, the area below the curve on the densification zone has occurred with less deformation and with an abrupt increase in stress (Figure 7a).The energy under the plateau area and the total area is:

$$W_{Plateau} = \int_0^{0,608} \sigma(\varepsilon)\, d\varepsilon = 2{,}256 \times 10^7 \frac{J}{m^3}$$

$$W_{Total} = \int_0^{0,843} \sigma(\varepsilon)\, d\varepsilon = 1{,}785 \times 10^8 \frac{J}{m^3}$$

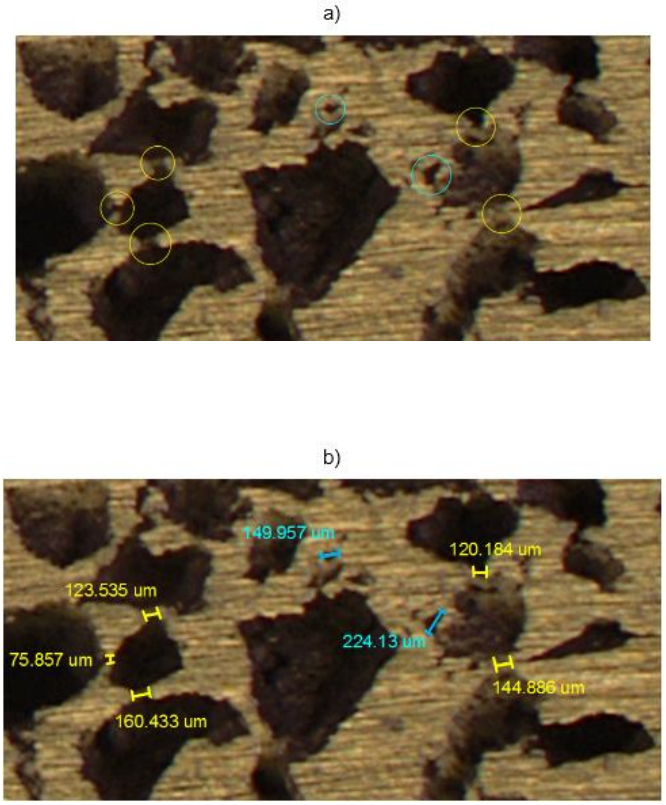

Figure6.Enlarged view of a photographic fraction of one of the samples, where the ducts connecting the pores with each other can be seen, resulting from the inter-granular contact

points between the NaCl particles (circles and yellow dimensions enclosing possible ducts seen longitudinally, circles and blue dimensions enclose possible transverse seen ducts: a) Identification of ducts, b) Ducts identified with their respective thickness measurements.

Confronting these two absorbed energies, it is observed that practically 87% of the total energy absorbed corresponds to the densification zone, which shows that this zone possesses the greatest capacity of energy absorption of the foam.

These results prove the extensive deformation energy absorption capacity of this type of material, which is mainly attributed to the adjustment of the porous mesh during the incidence of stress. (Fernández, Cruz, & García, 2009).

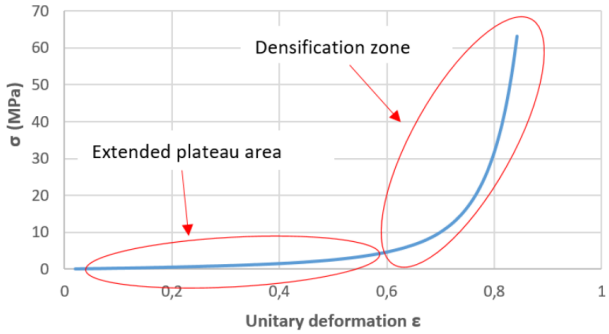

Figure7.Stress-strain of the open-cell metal foam specimen.

4. CONCLUSIONS

In this research it has been possible to obtain metallic foams of open cell by the infiltration method in soluble performs (the soluble perform used was NaCl).The evidence of the open structure is clearly seem in Figure 6 where interconnectivity between pores is evident. This interconnectivity is an indispensable requirement for the NaCl grains to be dissolved, otherwise they would be isolated and therefore trapped in the metal.

The open cell metal foams that were obtained by the infiltration method have an average relative density of 0.145, which leads to a high degree of porosity with a mean value of 85.5% (Table 1).One of the reasons for achieving this porosity could be the finer particles used (0.85 - 1.7 mm) compared with other authors (1.4 - 1.7 mm)(Luna, Barari, Woolle, & Goodall, 2014), in which the average value of porosity is 63.2% (ie a relative density of 0.368).

As far as the structural characterization is concerned, within the studied parameters, only the pore-per-inch distribution (PPI) shows a uniform behavior. Thickness of ligaments, surface pore

size, pore length and width present values in broad ranges with high levels of standard deviations.

The pores that contributes to an isotropic behavior to the foam are approximately only 21.02%, they are in a width / long ratio range of 0.8-1, with a standard deviation of 11.89%.These results indicate that the amount of anisotropic pores, far exceeds those isotropic ones. Therefore, it is considered that the foams would present an anisotropic behavior. In addition, the pores appear to be extended in the direction of infiltration (90 ° to 150 ° from horizontal section of samples). It is estimated that in the direction of infiltration the foam will have higher levels of stiffness. However, more research is needed in this topic for a final conclusion.

During the structural characterization of the samples, it was observed that there are certain pores with sizes above the range of NaCl particle size (0.85-1.7 mm) used in the experiment. This may have occurred because the temperature during processing exceeded the melting temperature of the salt (801 ° C) at some regions, causing the sintering of NaCl particles, and resulting in the formation of agglomerates.

During the structural characterization of the samples, very small pores were also observed, which are below the range of particle size used in the experiment (0.85 mm); these could be points of contact between grains of salt, the same ones that after the dissolution of NaCl, allow the interconnection between pores. Some small particles could have overcome the sieving process at the minimum value (0.85 mm). Another very likely cause could be the degree of humidity of the NaCl, this because, when the temperature rises, steam can be generated, and this be trapped in the metal.

In the compression test, the stress-strain curve obtained clearly shows the extended plateau and densification zones. The observed behavior is similar to the curves shown by other authors(Ashby, et al., 2002).The elastic zone could not be defined because it has very small values of stress and strain. The difficulty of placing an strain gage over a metal foam contribute to the lack of information in this zone. The extended plateau zone has a slight positive slope, characteristic of this type of materials, which may be the result of the constant deformation hardening of the foam, due to the rearrangement of its structure during the deformation process.

Almost 87% of the total compressive energy absorbed corresponds to the densification zone of the stress–strain diagram. This means that during the densification step of the foam, a high capacity of impact absorption is guaranteed. The values obtained from the calculation of absorbed compressive energy, verify the high capacity of absorption of energy of deformation of this kind of materials, which is attributed mainly to the rearrangement of porous mesh during the incidence of the compressive force.

REFERENCES

[1]. Ashby, M., Evans, A., Fleck, N., Gibson, L., Hutchinson, J., & Wadley, H. (Febrero de 2002). *Metal Foams: a Design Guide*. Cambridge: Butterworth-Heinemann.

[2]. Banhart, J. (Junio de 2000). Artículo científico: *Manufacture, characterisation and application of cellular metals and metal foams*. Bremen, Germany: Pergamon.
[3]. Cruz, P., Fernández, L., & Coleto, J. (Septiembre de 2008). *Procesos de fabricación de metales celulares. Parte I: Procesos por vía líquida*. Medellin, Colombia: Revista Metalurgica.
[4]. Cruz, P., Fernández, L., & Coleto, J. (Marzo de 2009). *Procesos de fabricación de metales celulares. Parte II: Vía sólida deposición de metales, otros procesos*. Medellín , Colombia: Revista Metalurgia.
[5]. Fernández, P. (Septiembre de 2007). *Fabrication of aluminium base cellular metals* . Pereira, Colombia: Universidad Tecnológica de Pereira.
[6]. Fernández, P., Cruz, L., & García, L. (01 de Diciembre de 2009). *Use of recycled aluminium for low cost production of metallic foams*. Madrid, España: Universidad Politécnica de Madrid.
[7]. Fernández, P., Daza, M., Oviedo, E., Ortega, C., & Cruz, J. (2009). *Estudio comparativo con base en el ensayo de comprensión de esponjas de aluminio obtenidas mediante infiltración de preformas solubles.*Cartagena, Colombia: Revista Latinoamericana de Metalurgia y Materiales.
[8]. Gibson, L., & Ashly, M. (2007). *Cellular Solids, structure and properties*. England: Cambridge University.
[9]. Gutiérrez, J., & Oñoro, J. (Septiembre de 2008). *Espumas de aluminio.Fabricación,propiedades y aplicaciones*. Madrid: Universidad Politécnica de Madrid.
[10]. Hussain, Z., & Suffin, N. (2011). *Microstructure and Mechanical Behaviour of Aluminium Foam Produced by Sintering Dissolution Process Using NaCl Space Holder* . Malaysia: Universiti Sains Malaysia.
[11]. Irausquin, I. A. (Febrero de 2012). Tesis Doctoral: *Caracterización mecánica de espumas metálicas y su aplicación en sistemas de absorción de energía*. Madrid: Universidad Carlos III de Madrid.
[12]. Laughlin, D., & Hono, K. (2014). *Physical Metallurgy*. Lausanne, Switzerland: Elsevier.
[13]. Luna, E., Barari, F., Woolle, R., & Goodall, R. (Diciembre de 2014). Artículo científico: *Casting Protocols for the Production of Open Cell Aluminum Foams by the Replication Technique and the Effect on Porosity*. Sheffield, England: University of Sheffield.
[14]. Nebreda, J. (Abril de 2014). Tesis Doctoral: *Optimización de la estructura celular en espumas de aluminio*. Valladolid: Universidad de Valladolid.
[15]. Roldán, D., & Angel, B. (2012). *II Encuentro de Investigación Formativa, Ingeniería Industrial Medellín*. Medellín: Editorial Universidad Pontificia Bolivariana.
[16]. Xiaoqing, C., Zhihua, W., Hongwei, M., Longmao, Z., & Guitong, Y. (2006). *Effects of cell size on compressive properties of aluminum foam*. Taiyhuan, China: Taiyuan University of Technology.